International Journal of Basic and Applied Sciences, 5 (4) (2016) 196-199

International Journal of Basic and Applied Sciences

Website: www.sciencepubco.com/index.php/IJBAS
doi: 10.14419/ijbas.v5i4.5739
Research paper

Photo-acoustic properties of nanoTiO2:Er

R. Palomino-Merino [1]*, R. Lozada-Morales [1], J. Martínez-Juárez [1], G. Juárez-Díaz [1], J. Carmona-Rodriguez [1], P. Del Angel [2], S. Jiménez-Sandoval [3], S. A. Tomas [3], O. Zelaya-Angel [3], V. M. Castaño [4 *]

[1] Benemérita Universidad Autónoma de Puebla. 14 Av. Sur y Av. San Claudio, Col. San Manuel. 72570 Puebla, México. aPosgrado en Física Aplicada, Facultad de Ciencias Físico-Matemáticas. BDepartamento de Dispositivos Semiconductores.
[2] Subdivisión Investigación Científica Aplicada, Instituto Mexicano del Petróleo, P.O. Box 14-805, México 07730 D.F.
[3] Centro de Investigación y de Estudios Avanzados del IPN. cLaboratorio de Investigación en Materiales, Unidad Querétaro, Apdo. Postal 1-798, Querétaro76001, México. dDepartamento de Física, P.O. Box 14-740, México 07360 D.F.
[4] Centro de Física Aplicada y Tecnología Avanzada, U.N.A.M Boulevard Juriquilla 3001 Santiago de Querétaro, Querétaro 76230.
**Corresponding author E-mail: palomino@fcfm.buap.mx, meneses@unam.mx*

Abstract

Nanocrystalline Er-doped TiO2 was prepared by sol-gel at room temperature. X-ray diffraction, photoacoustic spectroscopy (optical absorption), transmission electron microscopy (TEM), and electron dispersion microscopy (EDS) were carried out on both as-prepared and thermally-annealed (air at 700 ºC) samples, revealing the anatase crystalline phase of TiO2. The samples exhibit an average grain size from 38 to 5.1 nm, as the nominal concentration of Er varies from 0 % to 7 %. The photoacoustic spectra evidence the absorption edge at 300 nm attributed to TiO2, as well as several electronic transitions which are atomic energy absorption-line levels characteristics of Er.

Keywords: *Titanium Dioxide; Crystal Morphology; Doping; Nanomaterials; Dielectric Materials Semicolon.*

1. Introduction

Titania (TiO_2) is a widely used due to its important optical, chemical and mechanical properties. Applications range from gas and/or humidity sensor, catalyst, optical coatings, to photovoltaic cells and rechargeable batteries, among many other [1-5]. To improve its optical performance, dye sensitization of TiO_2 has been performed towards a more efficient harvesting of optical energy, by absorbing light within a wider electromagnetic range [6-9]. Nanocrystalline TiO_2 represents an important alternative for most of the aforementioned applications and the sol–gel technique offers a suitable and economic route in the synthesis of TiO_2 [10], [11] and, most important, the synthesis of titania with adequate optical probes included in the bulk.
Accordingly, in this work nanocrystalline Er-doped TiO_2 synthetized by sol-gel from titanium isopropoxide (Ti $(OC_3H_7)_4$) as precursor, with thermal annealing in air, is reported. Physical properties of the nanotitania are discussed as function of the Er content and particle size. This material has potential applications photocatalysis and energy storage, as shall be discussed.

2. Experimental

Nanocrystalline titania (NT) was prepared by mixing, at room temperature (RT), 1.0 mol of titanium isopropoxide (TIPO) (Aldrich) with 2.0 mol of acetic acid (Aldrich) and 2.0 mol of isopropanol (Baker) under stirring. Separately, 0.5 mol of $Er(NO_3)_3.3H_2O$ (Aldrich) was dissolved in a mixture of 2.0 mol of water, 2.0 mol of propanol and 2.0 mol of acetic acid. Subsequently, both solutions were mixed under vigorous agitation. Titania sols doped with 0.01, 0.03, 0.04, 0.05, 0.06 and 0.07 molar concentrations of Er were so obtained. After two months of gelation the samples were thermally annealed in air at 700 ºC for 1 hour.
A Siemens D-5000 powder diffractometer using the CuK_α radiation was employed. Optical absorption was measured with a home-made photoacoustic spectrometer, equipped with a Xe lamp (Oriel), a monochromator (Oriel), a mechanical chopper (Oriel) held at 17 Hz, and a closed photoacoustic cell. A D/Max2100 Rigaku Transmission Electron Microscopy (TEM) was used. Semi-quantitative measurements of atomic concentration of Ti, O, and Er elements were achieved by electron dispersion spectroscopy (EDS), utilizing a Voyager II X-ray quantitative microanalysis in an 1100/1110 EDX system, from Noran Instruments.

3. Results and discussion

The atomic percentage (at %) of Er in $nTiO_2$, measured by EDS, vs. the nominal concentration (in percentage units) of Er [NEr] in the growing solution is displayed in Fig. 1.

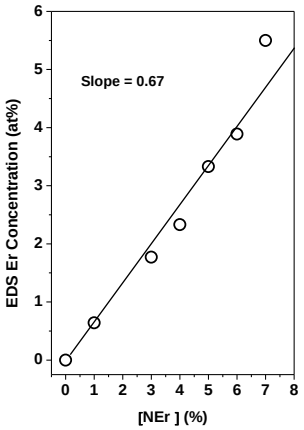

Fig. 1: EDS Measured Concentration of Er vs. Nominal [Ner] Concentration of Er in the Growing Precursor Solution.

A linear behavior is observed for the whole range of [NEr] studied. The solid line represents the linear least square fitting to the data. The slope of the straight line is 0.67 ± 0.04, which indicates that, in general, only 2/3 of the nominal Er percentage is observed in each sample. The remaining 1/3 is probably sublimated during the gelation and/or the thermal annealing at 700 ºC. Figure 2 shows the X-ray diffraction (XRD) patterns, in the 2θ range 10º - 75º of all the samples. The material exhibits the anatase crystalline structure of TiO_2; some peaks reveal the presence of small amounts of rutile and brookite phases of TiO_2, only in the undoped sample [12].

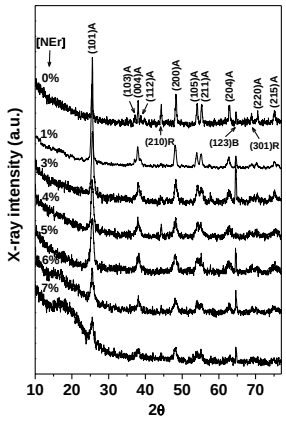

Fig. 2: X-Ray Diffraction Patterns for All the [Ner] Contents. A, B and R Letters Attached to the Indexes on XRD-Peaks Denotes Anatase, Brookite And Rutile, Respectively.

Reflections due to Er and Er-oxides were not observed, as in $nTiO_2$: Er nanoparticles reported by other authors [13]. The XRD peaks broaden with the Er content, which is consequence of the size reduction of particles as more Er is incorporated into the TiO_2. Figure 3 shows a typical TEM image of the $nTiO_2$ prepared with 5 % [Er] sample, revealing an averge grain size of 5 nm.

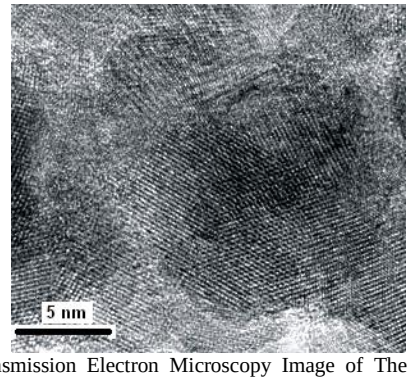

Fig. 3: Transmission Electron Microscopy Image of The Sample with [Ner] = 5 at %. The Black Bar at the Down-Left Corner Corresponds to 5 Nm.

The optical absorption (OA) spectra, measured by using photoacoustic (PA) spectroscopy, in the range 1.5 – 4.0 eV range, are presented in Figure 4 for all the samples.

The advantage of using the PA spectroscopy for OA measurements is that it is less sensitive to light scattering effects than conventional optical techniques [14]. The spectra evidence an absorption edge at a wavelength of around 3.0 eV and six electronic transitions, which indicate some well-defined Er atomic energy absorption levels. The six electronic transitions, identified with triply ionized erbium ions, are $^4I_{9/2}$, $^4F_{9/2}$, $^4S_{3/2}$, $^2H_{11/2}$, and $^4F_{3/2}$, all of them are transitions until the ground level $^4I_{15/2}$ [15]. The inset in Figure 4 displays how the $^4S_{3/2}$ level is resolved from the $^2H_{11/2}$ by a deconvolution procedure.

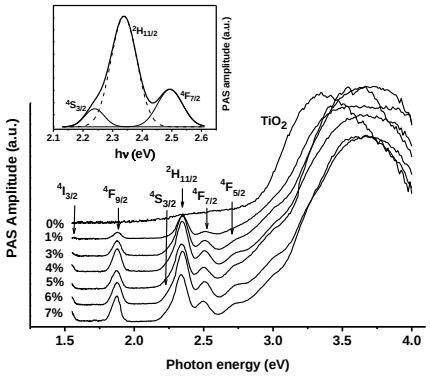

Fig. 4: Photoacoustical Optical Absorption Spectra (PAS) for All the [Ner] Values Analyzed. the Inset Describes the Deconvolution Process Applied to Resolve the $^4S_{3/2}$ and $^2H_{11/2}$ Emissions.

Figure 5 exhibits the nanoparticle average grain size (GS) as a function of [NEr], calculated from the Scherrer formula by considering, as an approximation, a spherical shape of the grains. It can be observed that GS decreases when [NEr] increases.

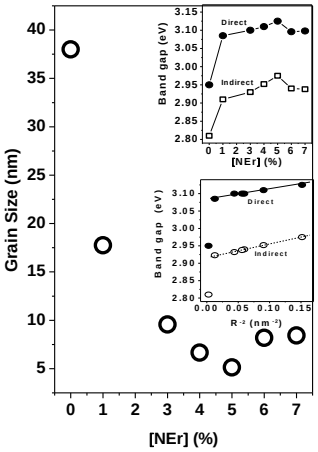

Fig. 5: Grains Size as a Function of [Ner]. The Top Inset Displays the Direct and the Indirect Energy Band Gaps Vs [Ner]. The Bottom Inset (A) Displays E_{gd} and E_{gi} Vs. The Inverse Radius Square of the Nanoparticle. the Solid and Dotted Lines are Least Square Fitting of the Data.

Bahtat and co-workers have suggested that Er^{3+} strongly affects the crystallization of sol-gel-based titania by stabilizing amorphous material [16]. Then, in our case, Er and thermal annealing of TiO_2 samples produced nanocrystalline grains, whose average diameter depended on [NEr] and on the annealing temperature values chosen that, in this work, was 700 ºC. A minimum value of GS is observed in Figure 5 for [NEr] = 5 %, whereas [NEr] = 6 and 7 % GS have higher values. This behavior indicates that GS does not follow a monotonically decrease as [NEr] increases. This could be related to a limited solubility of Er in TiO_2 since, due to this effect, Li and co-workers [17] have reported that for Er around 3 at% in TiO_2 other phases of Ti, O and Er arise. In our samples no other phases of TiO_2 were observed, so probably in our

case that limit of solubility occurs around [NEr] ~ 5 % (3.3 at% measured by EDS according to Figure 1) and for [NEr] > 5 % no more Er ions enter into the nanocrystalline lattice of TiO_2. For [NEr] = 6 and 7 % amorphous material composed by Ti, O, and Er elements, aside from crystalline TiO_2:Er, can be present into the nanoparticle, as suggested by the broad band observed at low 2θ values for these two values of [NEr].

The direct (E_{gd}) and indirect (E_{gi}) forbidden energy band gaps of TiO_2:Er nanoparticles were calculated by employing the relation $(\alpha h\nu)^n \propto (h\nu - E_g)$, n = 1/2 for the indirect band gap and n = 2 for the direct one. Here, α is the optical absorption coefficient, and hν is the photon energy. Taking into account that under the conditions studied in this work the PA amplitude is directly proportional to α, the relation $(\text{PA amplitude}*h\nu)^n \propto (h\nu - E_g)$ can be employed to calculate E_{gd} and E_{gi}. The top inset in Fig. 5 displays the E_{gd} and E_{gi} versus the nominal concentration of Er, for all the [NEr] values. It can be observed that E_{gd} and E_{gi} show minima for [NEr] = 5 %, as expected, because the lowest R is obtained when [NEr] = 5 %. In the bottom inset, E_{gd} and E_{gi} vs. quadratic inverse of the radius (R) of the particle is plotted. It can be seen that E_{gd} and E_{gi} follows the theoretically predicted linear dependence on R^{-2}. This quantum confinement occurs in the weak confinement region, since the Bohr radius of anatase is 0.8 nm [18]. The solid and dotted lines in the top inset is the result of the E_g vs. R^{-2} linear fitting of the E_{gd} and E_{gi} data, respectively. It is important to remark that the undoped TiO_2 has experimental E_{gd} and E_{gi} values very different from the values predicted by the solid line. This suggests that the nanometric character of the TiO_2: Er material, with its respective quantum confinement effects, is mainly originated by the incorporation of Er in the TiO_2 lattice.

The area under the absorption bands, calculated from fitting Gaussian functions, as illustrated in the inset of Figure 4, corresponding to the $^4S_{3/2}$, $^2H_{11/2}$, and $^4F_{3/2}$ transitions as a function of nanoparticle radius (R) and as a function of the [NEr], is plotted in Figure 5 and the inset, respectively. The area under each band is proportional to the number of photons absorbed at around the energy of the transition. The light absorption in these bands improves if [NEr] increases, as expected. However, saturation is observed for larger [NEr] values. Saturation can come from the limited solubility of Er in crystalline TiO_2.

On the other hand, as a consequence of the results shown in the inset of Figure 6, the band-area vs. R of Figure 6, maxima absorption values for R = 3 and 4 nm are observed, in the three transitions analyzed. If optical absorption is maximum for these R values, larger light emissions could be expected for TiO_2:Er nanoparticles with radius in the 3 - 4 nm interval.

4. Conclusions

Reproducible nanocrystalline Er-doped TiO_2 was prepared by sol-gel. The average diameter of the nanoparticles depends on the Er concentration incorporated into the TiO_2 lattice. The Er concentration in the nanocrystalline TiO_2 is around 2/3 of the Er nominal concentration in the growing precursor solution. The direct and indirect band gap energies depend on the size of the particle, approximately following the well-known E_g versus R^{-2} linear dependence. Photoacoustic spectra evidence the $^4I_{9/2}$, $^4F_{9/2}$, $^4S_{3/2}$, $^2H_{11/2}$, and $^4F_{3/2}$, electronic transitions of Er^{3+} ions. Analysis of area under the $^4S_{3/2}$, $^2H_{11/2}$, and $^4F_{9/2}$ bands is discussed in terms of the Er concentration in TiO_2 nanoparticles.

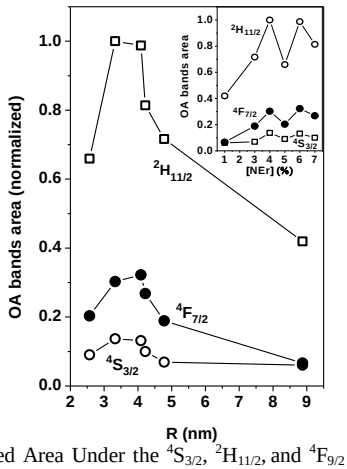

Fig. 6: Normalized Area Under the $^4S_{3/2}$, $^2H_{11/2}$, and $^4F_{9/2}$ Transitions Absorption Bands Versus the Radius of the Tio_2: Er Nanoparticles. The Inset Displays the Area Under Bands as A Function of [Ner].

References

[1] Yan Y, Chaudhuri SR, Chen DG & Sarkar A (1995), Sol- Gel Synthesis of Titania Thin-Film-Stabilized Porous Silica Coating. Chemistry of Materials 7, 2007-2009. http://dx.doi.org/10.1021/cm00059a006.

[2] Gusamano G, Montesperelli G, Nuziante P, Traversa E, Montenero A, Braghini M, Mattogno G & Bearzotti A (1993), Humidity-Sensitive properties of Titania Films Prepared using the Sol-Gel Process. Journal of Ceramic Society of Japan 101[9], 1095-1100. http://dx.doi.org/10.2109/jcersj.101.1095.

[3] Hamasaki Y, Ohkubo S, Murakami K, Sei H & Nogami G (1994), Photoelectrochemical Properties of Anatase and Rutile Films Prepared by the Sol-Gel Method. Journal of the Electrochemical Society 141[3], 660-663. http://dx.doi.org/10.1149/1.2054787.

[4] Bahtat A, Bouazaoui M, Bahtat MM, Garapon C, Jacquier B & Mugnier J (1996), Up-conversion fluorescence spectroscopy in Er3+: TiO2 planar waveguides prepared by a Sol-Gel process. Journal of Non-Crystalline Solids 202, 16-22. http://dx.doi.org/10.1016/0022-3093(96)00172-X.

[5] Huang SY, Kavan L, Exnar I & Grätzel M (1995), Rocking chair Lithium battery based on nanocrystalline TIO2 (Anatase). Journal of the Electrochemical Society 142, 142-144. http://dx.doi.org/10.1149/1.2048726.

[6] Tomás SA, Stolik S, Palomino R, Lozada R, Persson C, Pepe I, & Ferreira da Silva A (2005), Influence of rhodamine 6G doping on the optical properties of TiO2 sol-gel films. Journal of Applied Physics 98, 073516. http://dx.doi.org/10.1063/1.2073972.

[7] Tomás SA, Stolik S, Palomino R, Lozada R, Persson C, Ahuja R, Pepe I, & Ferreira da Silva A (2005), Optical properties of rhodamine 6G-doped TiO2 sol-gel films. Journal de Physique IV 125, 415-417. http://dx.doi.org/10.1051/jp4:2005125097.

[8] Tomás SA, Palomino R, Lozada R, da Silva Jr EF, de Vasconcelos EA, de Azevedo WM, Persson C, Pepe I, David DGF, & Ferreira da Silva A (2005), Optical and Electronic Characterization of the Band Structure of Blue Methylene and Rhodamine 6G-doped TiO2 Sol-Gel Nanofilms. Microelectronics Journal 36, 570-573. http://dx.doi.org/10.1016/j.mejo.2005.02.093.

[9] Ferreira da Silva A, Pepe I, Gole JL, Tomás SA, Palomino R, de Azevedo WM, da Siva Jr EF, Ahuja R & Persson C (2006), Optical properties of in situ doped and undoped titania nanocatalysts and doped titania sol-gel nanofilms. Applied Surface Science 252, 5365-5367. http://dx.doi.org/10.1016/j.apsusc.2005.12.041.

[10] Komuro S, Katsumata T, Kokai H, Morikawa T & Zhao X (2002), Change in photoluminescence from Er-doped TiO2 thin films induced by optically assisted reduction. Applied Physics Letters 81, 4733-4735. http://dx.doi.org/10.1063/1.1530733.

[11] Gaponenko NV, Sergev OV, Stepanova EA, Parkun VM, Mudryi AV, Gnaser H, Misiewicz J, Heiderhoff R, Balk LJ, & Thompson GE (2001), Optical and Structural Characterization of Erbium-Doped TiO2 Xerogel Films Processed on Porous Anodic Alumina. Journal of the Electrochemical Society 148[2], H13-H16. http://dx.doi.org/10.1149/1.1339864.

[12] Anatase: PDF # 73-1764. Rutile: PDF # 78-1509. Brookite: PDF # 76-1936.

[13] Jeon S & Braun P (2003), hydrothermal synthesis of Er-doped luminescent TiO2 nanoparticles. Chemistry of Materials 15, 1256-1263. http://dx.doi.org/10.1021/cm0207402.

[14] Toyoda T & Tsuboya I (2003), apparent band-gap energies of mixed TiO2TiO2 nanocrystals with anatase and rutile structures characterized with photoacoustic spectroscopy. Review of Scientific Instruments 74, 782-784. http://dx.doi.org/10.1063/1.1512984.

[15] Kaminskii AA (1990), Laser Crystals: Their Physics and Properties, Springer-Verlag, pp 10. http://dx.doi.org/10.1007/978-3-540-70749-3.

[16] Bahtat A, Bouderbala B, Bahtat M, Boauzaoui M, Mugnier J & Druetta M (2006), Structural characterization of Er3+ doped sol–gel TiO2 planar optical waveguides. Thin Solid Films 506/507, 59-62.

[17] Li J-G, Wang X-H, Kamiyama H, Ishigaki T, & Sekiguchi T (2006), RF plasma processing of Er-doped TiO2 luminescent nanoparticles. Thin Solid Films 506/507, 292-296. http://dx.doi.org/10.1016/j.tsf.2005.08.093.

[18] Elim HI, Ji W, Yuwono AH, Xue JM, & Wang J, (2003), Ultrafast optical nonlinearity in poly(methylmethacrylate)-TiO2poly(methylmethacrylate)-TiO2 nanocomposites. Applied Physics Letters 82, 26913693. http://dx.doi.org/10.1063/1.1568544.